Geophysical Research Letters

RESEARCH LETTER
10.1029/2019GL086321

Relative Contributions of Atmospheric, Oceanic, and Coupled Processes to North Pacific and North Atlantic Variability

Timothy A. Myers[1,2] **and Carlos R. Mechoso**[2]

[1]Lawrence Livermore National Laboratory, Livermore, CA, USA, [2]Department of Atmospheric and Oceanic Sciences, University of California, Los Angeles, CA, USA

Key Points:
- Anomalous energy budget of ocean mixed layer associated with North Pacific and North Atlantic variability is quantified.
- Mechanisms for interannual sea surface temperature variability over northern oceans exhibit pronounced geographic dependence.
- Anomalous cloud radiative flux is an order one process for subtropical northeast Pacific variability.

Supporting Information:
- Supporting Information S1

Correspondence to:
T. A. Myers,
myers74@llnl.gov

Citation:
Myers, T. A., & Mechoso, C. R.. (2020). Relative contributions of atmospheric, oceanic, and coupled processes to North Pacific and North Atlantic variability. *Geophysical Research Letters*, *47*, e2019GL086321. https://doi.org/10.1029/2019GL086321

Received 18 NOV 2019
Accepted 19 FEB 2020
Accepted article online 21 FEB 2020

Abstract Patterns of sea surface temperature (SST) variability over the northern oceans arise from a combination of atmospheric, oceanic, and coupled processes. Here we use a novel methodology and a suite of observations to quantify the processes contributing to the dominant patterns of interannual SST variability over these regions. We decompose the upper ocean heat content tendency associated with such dominant patterns into contributions from different heat fluxes: (a) atmospherically driven, (b) surface feedbacks, and (c) oceanic. We find that in the subtropics, cloud radiative flux, turbulent heat flux, and residual oceanic processes each contributes substantially to North Pacific SST variability, whereas turbulent heat flux primarily induces North Atlantic SST variability. Cloud radiative fluxes therefore provide a major source of interannual SST variability in the North Pacific but not in the North Atlantic. In midlatitudes, SST fluctuations over the northern oceans are driven by the combination of turbulent and oceanic heat fluxes.

Plain Language Summary The surface temperature of the North Atlantic and North Pacific oceans naturally varies from 1 year to the next in a spatially coherent manner. This variability originates from processes in the atmosphere and ocean, as well as from atmosphere-ocean interactions. In this investigation, we use observational data to quantify these processes, which enables us to discern their relative contributions in generating year-to-year sea surface temperature fluctuations. Our results show that variations in clouds, through their influence on the sunlight absorbed by the ocean, are as important as other mechanisms for sea surface temperature fluctuations in the subtropical North Pacific. By contrast, clouds' impact in the subtropical North Atlantic is small. We find that in the midlatitudes of both ocean basins, sea surface temperature changes are primarily induced by variations in surface winds that modify the exchange of heat between the ocean and atmosphere and that alter ocean circulation patterns.

1. Introduction

Both the North Pacific and Atlantic Oceans exhibit coherent patterns of sea surface temperature (SST) variability on interannual-to-interdecadal timescales. Wind-driven surface heat fluxes induced by random fluctuations in the atmospheric circulation are responsible for a large portion of such SST variability (e.g., Battisti et al., 1995; Cayan, 1992; Deser et al., 2010; Frankignoul & Hasselmann, 1977). It has even been suggested that the dominant pattern of North Atlantic SST variability, the Atlantic Multidecadal Oscillation (AMO), is almost exclusively driven by this weather "noise" (Clement et al., 2015). The dominant pattern of SST variability in the North Pacific, the Pacific Decadal Oscillation (PDO), arises from a superposition of several processes: (a) anomalous surface heat fluxes and Ekman transport due to midlatitude weather noise and teleconnections from the tropics, (b) ocean memory, and (c) oceanic Rossby wave propagation (Newman et al., 2016).

There is abundant evidence from observational data and numerical model results that an atmosphere-ocean coupled process consisting of a locally positive cloud radiative feedback over eastern subtropical and northern midlatitude oceans locally amplifies the magnitude and persistence of SST anomalies associated with the PDO and AMO (hereafter referred to as North Pacific variability and North Atlantic variability; Bellomo et al., 2014, 2016; Brown et al., 2016; Burgman et al., 2008, 2017; Clement et al., 2009; Deser et al., 2004; Myers, Mechoso, & DeFlorio, 2018; Norris et al., 1998; Yuan et al., 2016, Yuan et al., 2018). This feedback acts to increase the damping timescale of SST anomalies. A few modeling studies estimate that the

feedback explains up to around 30% of the amplitude of SST anomalies associated with North Pacific and North Atlantic variability in the subtropics (Bellomo et al., 2016; Burgman et al., 2017). However, the role of this coupled process and of cloud radiative fluxes relative to other mechanisms for the generation of the SST anomalies associated with these patterns of variability has not been rigorously quantified using observations. Myers, Mechoso, Cesana, et al. (2018) used observations to investigate the mechanisms responsible for the exceptionally warm SST anomalies off Baja California in 2014 and 2015 that exhibited a pattern very similar to the warm phase of North Pacific variability. By quantifying the upper ocean energy budget, they found that a reduction in marine boundary layer clouds and commensurate increase in solar radiation absorbed by the ocean was the dominant process that produced such a "marine heatwave." Here we generalize and refine the methods of Myers, Mechoso, Cesana, et al. (2018) in order to quantify and understand the atmospheric, oceanic, and coupled processes underlying interannual SST changes associated with the dominant patterns of variability over the North Pacific and North Atlantic.

2. Data and Methods

Using primes to denote anomalies from climatological monthly means, we decompose the observed anomalous heat content tendency of the oceanic mixed layer at each 1° by 1° grid box and month as

$$\left(\rho c_p h \partial T/dt\right)' = F'_{turb} + F'_{cloud} + F'_{clear} - \left(\rho c_p h(\boldsymbol{V}\cdot\nabla T)\right)' + RES'. \quad (1)$$

Here, T is SST and $\boldsymbol{V}$ is vertically averaged horizontal velocity in the mixed layer of depth h. The first three terms on the right hand side of equation ((1)) represent anomalous surface heat fluxes by turbulence, including sensible plus latent heat contributions $\left(F'_{turb}\right)$, net (downwelling minus upwelling) cloud-induced radiation (F'_{cloud}), and net clear-sky radiation (F'_{clear}). Also, $\rho = 1{,}025$ kg/m^3 is the density of seawater and $c_p = 3{,}994$ J/kg/K is the specific heat of seawater at constant pressure. The term RES' in equation ((1)) is a residual flux that closes the budget and is inferred to represent vertical mixing at the base of the mixed layer. A simplified form of equation ((1)) is written as

$$\left(\rho c_p h \partial T/dt\right)' = F'_{turb} + F'_{rad} + F'_{ocean}, \quad (2)$$

where $F'_{rad} = F'_{cloud} + F'_{clear}$ is the anomalous net all-sky radiative flux and $F'_{ocean} = -\left(\rho c_p h(\boldsymbol{V}\cdot\nabla T)\right)' + RES'$ is the anomalous total oceanic heat flux into the mixed layer due to horizontal advection and vertical mixing.

In our calculations, we take observation-based estimates of h and horizontal velocity from the National Centers for Environmental Prediction Global Ocean Data Assimilation System (Behringer, 2007; Behringer & Xue, 2004). T is taken to be SST from the National Oceanic and Atmospheric Administration (NOAA) Optimum Interpolation (OI) SST data set V2 (Reynolds et al., 2002). $\boldsymbol{V}$ is defined as the vertically averaged horizontal velocity spanning all levels (given at 10-m resolution) within the mixed layer. The temperature tendency $\partial T/\partial t$ is approximated at each month t as T for the subsequent month subtracted by T for the previous month, divided by 2 months. $\boldsymbol{V}\cdot\nabla T$ is approximated using centered finite differencing in spherical coordinates.

We obtain F_{cloud} and F_{clear} from the satellite-based Clouds and the Earth's Radiant Energy System (CERES) Energy Balanced and Filled (EBAF) data set version 4 (Kato et al., 2018), which is widely considered to produce the most state-of-the-art gridded observational estimates of surface radiative fluxes. F_{cloud} is the cloud radiative effect, defined as net (downwelling minus upwelling) all-sky minus clear-sky radiation at the surface. A major advantage of surface flux data from CERES-EBAF is that it is constrained by satellite measurements of radiation at the top of the atmosphere, unlike reanalyses or other satellite-based data sets such as the International Satellite Cloud Climatology Project Flux product (Zhang et al., 1995). Additionally, surface fluxes in CERES-EBAF are estimated based on state-of-the-art satellite cloud retrievals from passive and active sensors, including the Moderate Resolution Imaging Spectroradiometer, Cloud–Aerosol Lidar and Infrared Pathfinder Satellite Observations, and CloudSat (Kato et al., 2018).

To reduce observational uncertainty in F_{turb}, this is computed as an ensemble mean across four observational data sets, including the Objectively Analyzed Air-sea Fluxes Project (OAFlux) (Yu et al., 2008), European Centre for Medium-Range Weather Forecasts Interim Re-Analysis (ERA-I) (Dee et al., 2011), Climate

Forecast System Reanalysis (CFSR) (Saha et al., 2010), and Modern-Era Retrospective Analysis for Research and Applications, version 2 (MERRA-2) (Gelaro et al., 2017). Assuming that biases across data sets are uncorrelated, averaging across data sets will reduce these biases. Evidence for this notion is presented in Bosilovich et al. (2009), who show that errors in precipitation and outgoing longwave radiation from an ensemble average of reanalyses are generally smaller than those from individual reanalyses. Similarly, the average across multiple climate models also tends to have smaller biases than those found in any one model (Gleckler et al., 2008).

The surface heat fluxes may be driven by factors unrelated to SST (thereby acting as a forcing) or respond to SST anomalies (thereby acting as a feedback). Thus, following Frankignoul and Kestenare (2002) (FK02), we further express F'_{turb} and F'_{cloud} as

$$F'_{turb} = (dF_{turb}/dT) \times T' + F^{*}_{turb}, \tag{3}$$

$$F'_{cloud} = (dF_{cloud}/dT) \times T' + F^{*}_{cloud}. \tag{4}$$

The first terms on the right-hand side of equations ((3)) and ((4)) are the components of F'_{turb} and F'_{cloud} that are linearly related to SST, which we call feedback-induced surface heat fluxes. The coefficients dF_{turb}/dT and dF_{cloud}/dT, referred to as surface heat flux feedbacks, are estimated directly from the data as in FK02 and previous analyses according to

$$dF_{turb}/dT = \frac{cov\left(T'_{-1}, F'_{turb}\right)}{cov\left(T'_{-1}, T'\right)}, \tag{5}$$

$$dF_{cloud}/dT = \frac{cov\left(T'_{-1}, F'_{cloud}\right)}{cov\left(T'_{-1}, T'\right)}, \tag{6}$$

where $cov()$ is the covariance operator and T'_{-1} is SST 1 month before T', F'_{turb}, and F'_{cloud} occur (Hausmann et al., 2016; Park et al., 2005). The second terms on the right-hand side of equations (3) and (4) are the components of F'_{turb} and F'_{cloud} that are not linearly related to SST, which we call surface heat flux forcings and compute as residuals.

Prior to the application of equations (5) and (6), variations in the surface flux and temperature anomalies with persistence times longer than 1 month should be removed in order to obtain unbiased feedback estimates (FK02). ENSO is a remote source of persistence. Hence, before applying equations (5) and (6), surface flux and temperature anomaly fields were linearly detrended; then the components of these anomalies related to the Niño 3.4 index (defined using detrended temperature anomalies) were removed by linear regression, following previous studies (FK02; Hausmann et al., 2016; Park et al., 2005).

Surface heat flux feedback estimates over the northern oceans are shown in supporting information Figure S1 and are qualitatively similar to those reported in previous results (FK02; Park et al., 2005). The turbulent heat flux feedback, dF_{turb}/dT, is negative north of ~10°N in both basins, indicating that this feedback damps SST anomalies, consistent with theoretical expectation and previous results. The cloud radiative feedback, dF_{cloud}/dT, is positive in the subtropical northeast (NE) Pacific and more weakly positive in the midlatitude North Pacific and midlatitude NE Atlantic, indicating that the feedback amplifies SST anomalies. This positive feedback arises due to reduced marine low cloud coverage with warmer SST and, by extension, reduced capping inversion strength, each of which enhances entrainment drying of the boundary layer (Bretherton et al., 2013; Klein et al., 2017; Klein & Hartmann, 1993; Rieck et al., 2012; van der Dussen et al., 2015).

We use the monthly mean PDO index from the Joint Institute for the Study of the Atmosphere and Ocean, University of Washington (http://research.jisao.washington.edu/pdo/PDO.latest.txt) to quantify the state of the dominant mode of North Pacific variability. An index defined as SST monthly anomalies averaged over 0°–60°N, 80°W–0° is used to quantify the state of the dominant mode of North Atlantic variability (as in Bellomo et al., 2016). We apply a 3-month running mean to each index to focus on SST variations on timescales of at least a season. We define the growth phase of North Pacific or North Atlantic variability as months when its corresponding index is positive and increasing (warm phase growth) or when its index is negative and decreasing (cold phase growth). The indices are determined to be increasing or decreasing based on

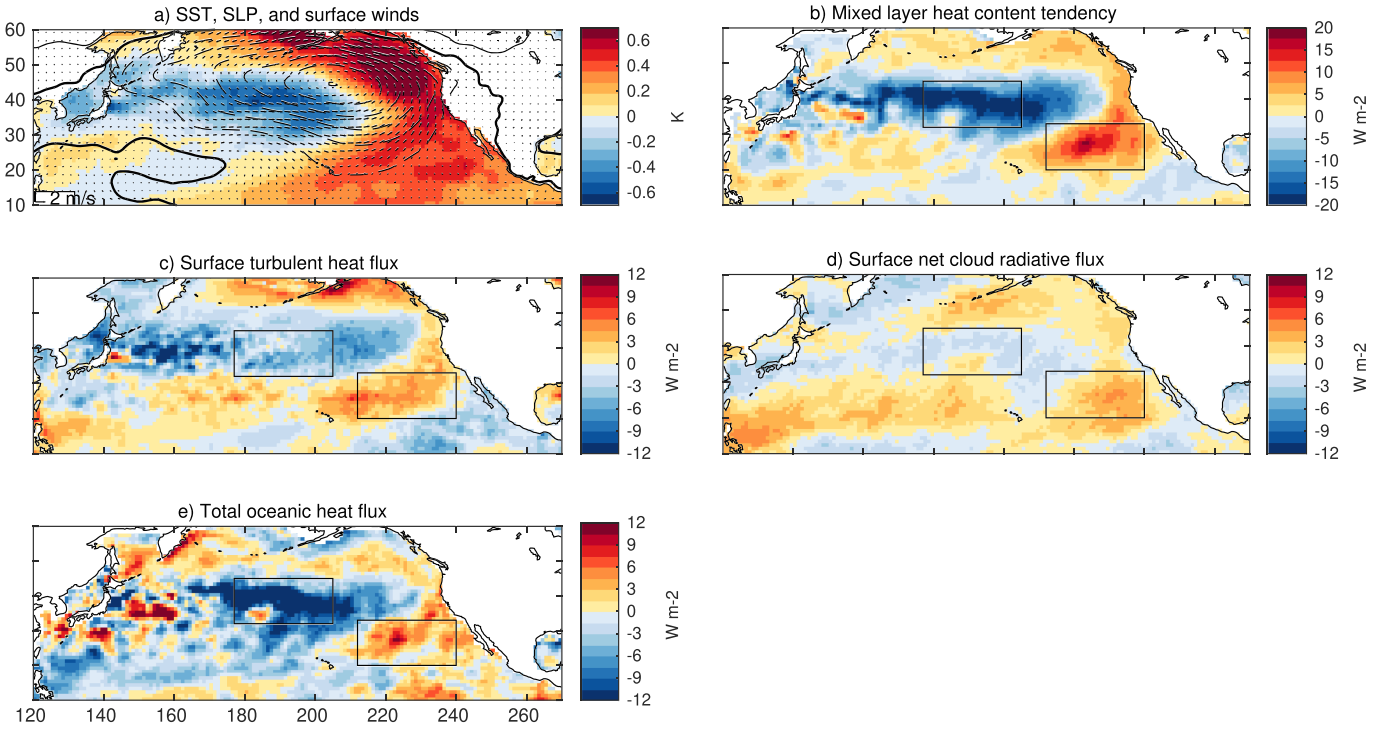

Figure 1. Average anomalous meteorological conditions and mixed layer energy budget components during the growth phase of North Pacific variability, including (a) NOAA OI SST, ERA-I SLP, and ERA-I near-surface winds; (b) $(\rho c_p h \partial T/dt)'$; (c) F'_{turb}; (d) F'_{cloud}; and (e) F'_{ocean}. Anomalies are relative to 2001–2016 climatological monthly means. Positive values indicate energy gained by the ocean. Maximum warming and cooling regions are outlined in black. SLP contours are in increments of 0.5 hPa, where the thick solid contour is the zero line separating negative (dashed contours) and positive (thin solid contours) anomalies.

the sign of their tendencies, computed using centered finite differencing. In order to discern mechanisms driving the growth of interannual SST anomalies, we compute the difference between the temporal average of each of the budget terms in equations (1)–(4) and meteorological fields for months experiencing warm phase growth and the temporal average of each term for months experiencing cold phase growth. We then take the mean of this sum, with weighting by the number of months that each condition is met. The resulting quantity represents an average anomalous mixed layer energy budget component or meteorological anomaly during the growth phase of North Pacific or North Atlantic variability.

Figure S2 displays time series of the two climate indices and SST anomalies in four target regions where, as we discuss in the next section, there are local maxima in the anomalous mixed layer heat content tendencies during the growth phases. The mean number of consecutive months when North Pacific variability is in its warm or cold phase (regardless of the tendency of its index) is 11, while the mean number of consecutive months when it is in its growth phase is 3. The corresponding mean numbers of consecutive months associated with North Atlantic variability are 12 and 3, respectively. This shows that each mode of variability persists in its warm or cold phase for around 1 year and exhibits pronounced interannual variability. Such a timescale is longer than that of the growth phase of variability of either mode because, after SST anomalies of a given warm or cold phase are amplified, those anomalies persist before being eroded by damping processes.

We select February 2000 to June 2017 to be the period of analysis because CERES-EBAF, the most reliable source of surface radiative flux we are aware of, does not extend further back in time. Thus, while the dominant modes of North Pacific and North Atlantic variability have interannual and interdecadal components, our analysis should only be considered as discerning mechanisms for interannual SST variability.

3. Mixed Layer Energy Budget of North Pacific Variability

Figure 1a shows SST, sea-level pressure (SLP), and near-surface wind anomalies during the growth phase of North Pacific variability. The canonical horseshoe pattern of anomalous SST characteristic of the warm

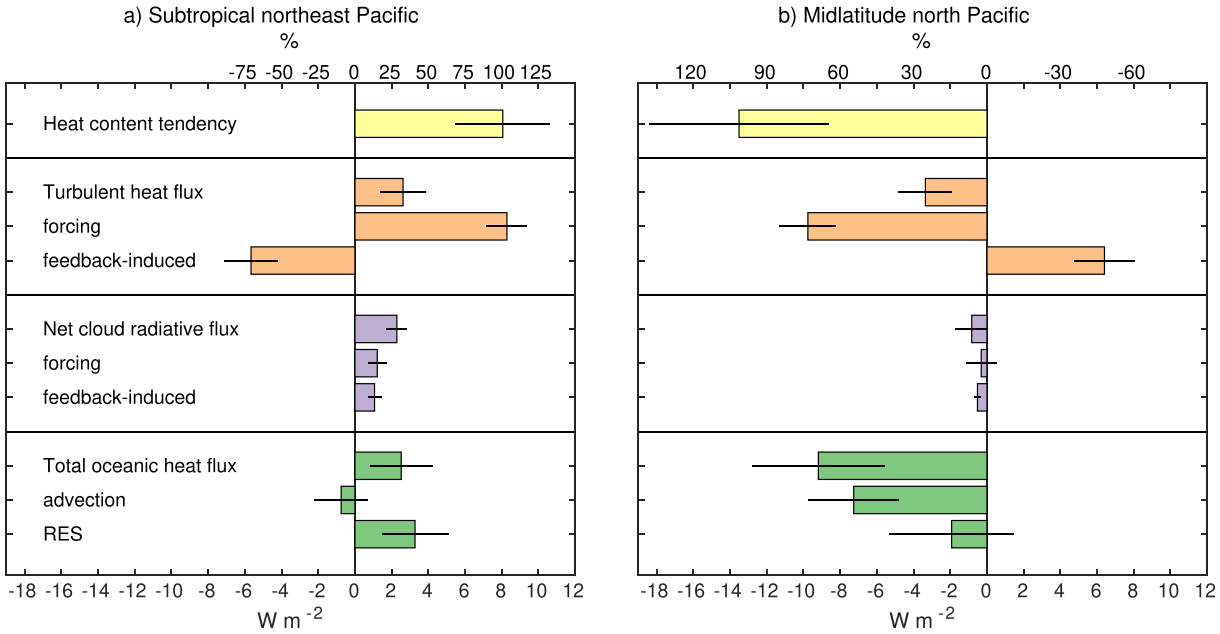

Figure 2. Spatial means of average anomalous mixed layer energy budget components during the growth phase of North Pacific variability over the (a) subtropical NE Pacific and (b) midlatitude North Pacific. Error bars are computed as in Myers, Mechoso, Cesana, et al. (2018) and span 90% sampling uncertainty using a two-tailed *t* test, taking into account spatial and temporal auto-correlation. Each error bar is proportional to the standard deviation of all monthly anomalies contributing to the spatiotemporal average of a given budget term; it includes information on the temporal and spatial variability of that budget term.

phase of the North Pacific variability is evident, along with an anomalous cyclonic circulation indicative of a strengthening of the Aleutian Low and weakening of the subtropical high. The anomalous mixed layer heat content tendency, $(\rho c_p h \partial T/dt)'$, typical of this growth phase shows a heating maximum in the warm subtropical NE Pacific (outlined by a rectangle, 20°N–33°N, 212°E–240°E) and cooling maximum in the cool midlatitude North Pacific (also outlined by a rectangle, 32°N–45°N, 177°E–205°E), amplifying the coincident SST anomalies (Figure 1b). F'_{turb}, F'_{cloud}, and F'_{ocean} during North Pacific variability's growth phase are shown in Figures 1c–1e. The pattern of F'_{turb} in Figure 1c is very similar to that of the heat content tendency and physically consistent with the surface wind anomalies, showing positive F'_{turb} in the subtropical NE Pacific where the trades weaken and negative F'_{turb} in the midlatitude North Pacific where the westerlies strengthen (see also Figure S3). The pattern of F'_{cloud} in Figure 1d shows positive F'_{cloud} in the subtropical NE Pacific, coincident with the maximum in positive heat content tendency anomalies and the region of climatologically abundant stratocumulus clouds. Anomalies are near-zero in the region of maximum negative heat content tendency anomalies in the midlatitude North Pacific. The values of F'_{clear} during the growth phase of North Pacific variability are near-zero and thus not shown. Finally, the pattern of F'_{ocean} in Figure 1e, like F'_{turb}, is very similar to that of the heat content tendency. However, F'_{ocean} is clearly maximum in the midlatitude North Pacific, indicating a fundamental role for oceanic processes for the growth of North Pacific variability in this region.

In order to understand the relative roles of atmospheric, oceanic, and coupled processes underlying North Pacific variability, next we spatially average over the outlined regions of the subtropical NE and midlatitude North Pacific all anomalous mixed layer energy budget components. From Figure 2a it is evident that in the subtropical NE Pacific, F'_{turb}, F'_{cloud}, and F'_{ocean} each contributes roughly equally to the anomalous heating of the mixed layer. Positive F'_{turb} is the result of positive turbulent heat flux forcing anomalies, F^*_{turb}, more than offsetting feedback-induced negative anomalies, $(dF_{turb}/dT) \times T'$, which on their own damp the warm subtropical NE Pacific SST anomalies. In contrast, positive F'_{cloud} is a result of reinforcing and approximately equally strong positive cloud radiative flux forcing anomalies, F^*_{cloud}, and feedback-induced positive anomalies, $(dF_{cloud}/dT) \times T'$. Finally, positive F'_{ocean} is almost entirely a result of residual oceanic flux, RES', and not

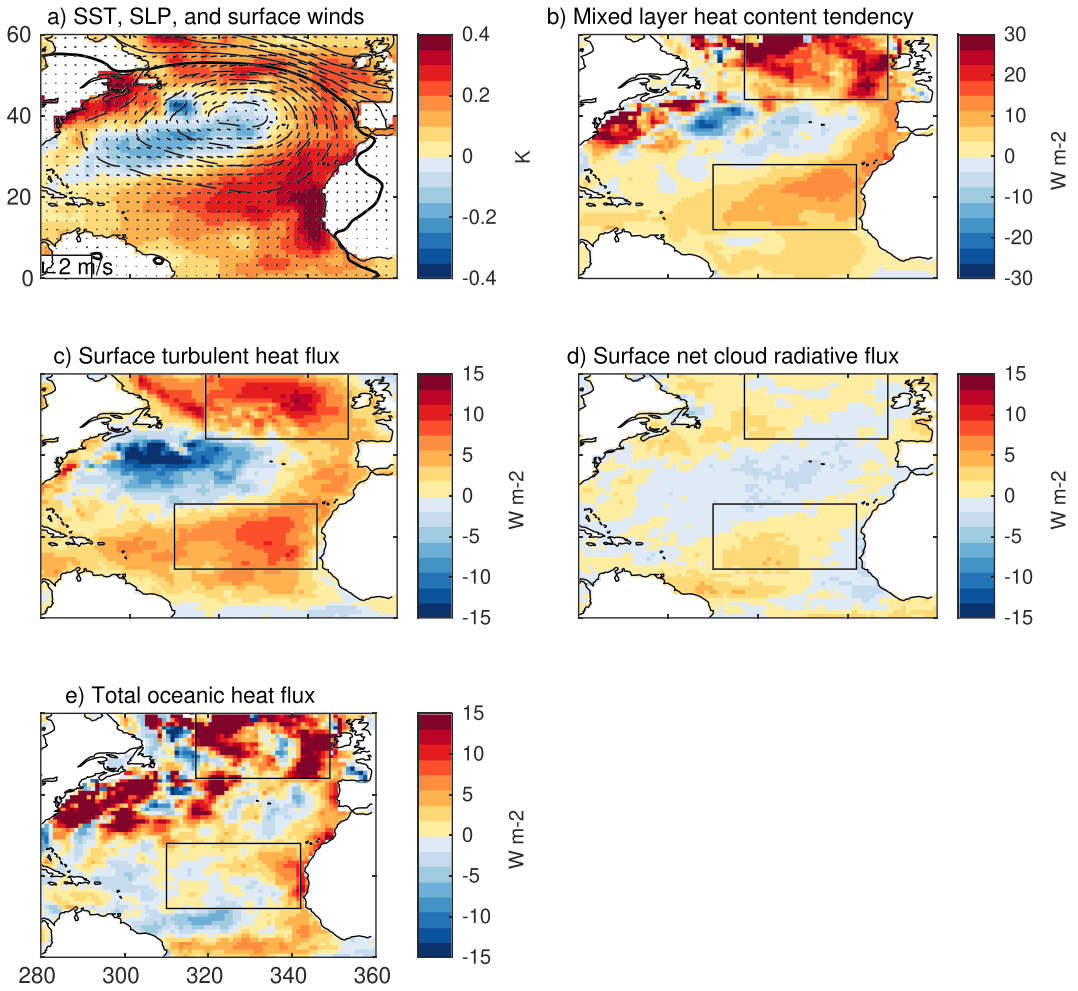

Figure 3. As in Figure 1 but for the growth phase of North Atlantic variability. Maximum warming regions are outlined in black.

horizontal advection, $-(\rho c_p h(\boldsymbol{V} \cdot \nabla T))'$, likely due to weaker-than-average vertical mixing at the base of the mixed layer and consistent with weaker trade winds' reducing ocean stirring.

From Figure 2b it is evident that in the midlatitude North Pacific, F'_{ocean} accounts for around 70% of the anomalous cooling of the mixed layer during North Pacific variability's growth phase. Negative F'_{ocean} is mostly a result of anomalous cold advection and consistent with stronger westerlies' enhancing Ekman transport from cooler northern waters. Negative F'_{turb} accounts for the overwhelming remainder of the mixed layer cooling and is a result of negative turbulent heat flux forcing anomalies more than offsetting feedback-induced positive anomalies that on their own damp the cool midlatitude North Pacific SST anomalies. We note that these results are largely insensitive to which turbulent flux data set is considered (Figure S4).

These findings show that the mechanisms for North Pacific interannual variability exhibit marked geographic dependence. Overall, surface turbulent heat flux, cloud radiative flux, and residual oceanic processes each contributes equally to subtropical NE Pacific heating typical of the growth phase of North Pacific variability. In contrast, oceanic processes—specifically advection—account for most of the midlatitude North Pacific cooling associated with the growth phase of North Pacific variability. Therefore, anomalous cloud radiative flux is an order one process for subtropical NE Pacific SST variability, accounting for on average around one third of anomalous mixed layer heat content tendency, but not for the midlatitude North Pacific. Moreover, around half of the subtropical NE Pacific cloud radiative flux is directly attributable to a cloud radiative feedback. These features are especially evident in the spatial patterns of the relative contributions of the individual heat fluxes to the local mixed layer heat content tendency (Figure S5).

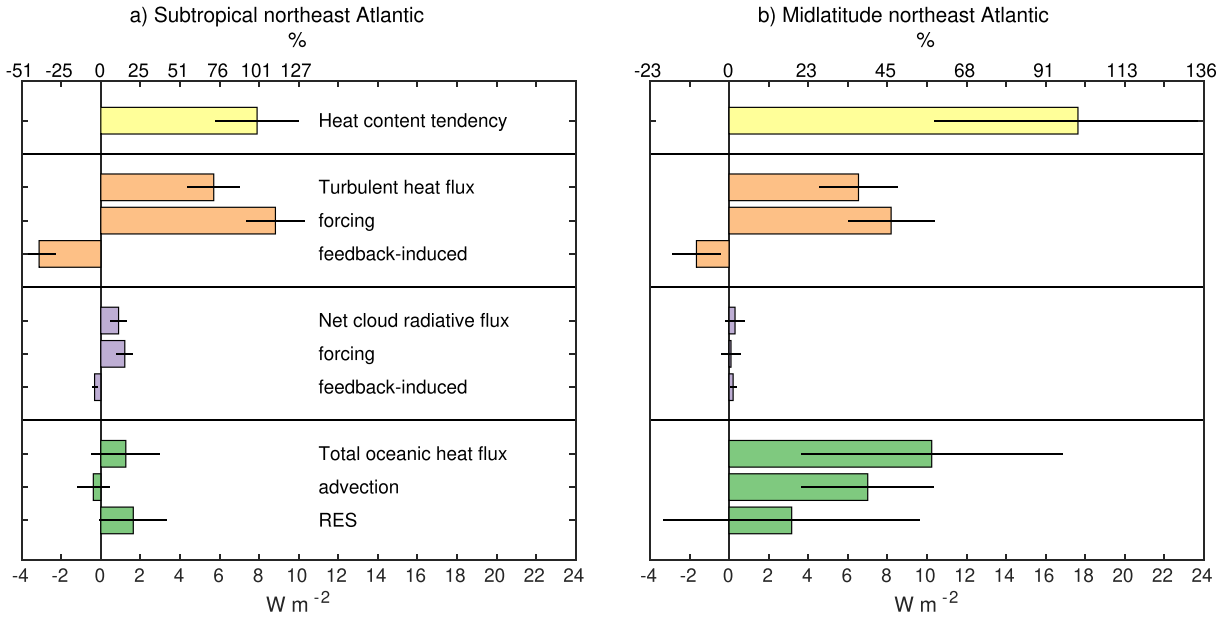

Figure 4. As in Figure 2 but for the growth phase of North Atlantic variability over the (a) subtropical NE Atlantic and (b) midlatitude NE Atlantic.

4. Energy Budget of North Atlantic Variability

Figure 3 shows the same quantities as in Figure 1 but for the anomalous atmospheric circulation and energy budget components during the growth phase of North Atlantic variability. The familiar pattern of anomalous SST and cyclonic circulation characteristic of the warm phase of North Atlantic variability is evident (Figure 3a). The anomalous mixed layer heat content tendency typical of this growth phase shows heating maxima in the warm subtropical NE Atlantic (12°N–28°N, 310°E–342°E) and midlatitude NE Atlantic (44°N–60°N, 317°E–349°E; Figure 3b). The pattern of F'_{turb} in Figure 3c is remarkably similar to that of the heat content tendency and physically consistent with the surface wind anomalies, showing positive F'_{turb} in the subtropical and midlatitude NE Atlantic where the background winds weaken (see also Figure S6). F'_{cloud} in Figure 3d is very slightly positive in the subtropical NE Atlantic and near-zero elsewhere. F'_{ocean} in Figure 3e exhibits a clear positive maximum in the midlatitude NE Atlantic, suggesting a fundamental role for oceanic processes for the growth of North Atlantic variability in this region.

Figure 4a shows that in the subtropical NE Atlantic, F'_{turb} accounts for around 70% of the anomalous heating of the mixed layer during North Atlantic variability's growth phase and is driven by strongly positive turbulent heat flux forcing. The remainder of the heating is roughly equipartitioned between small positive anomalies in F'_{cloud}, dominated by heat flux forcing, and F'_{ocean}, dominated by residual oceanic processes. In the midlatitude NE Atlantic, roughly 60% of the midlatitude warming is driven by F'_{ocean}, which is mostly a result of anomalous warm advection and consistent with weaker westerlies' reducing Ekman transport from cooler northern waters (Figure 4b). F'_{turb} accounts for nearly 40% of the anomalous warming of the mixed layer and is driven by strongly positive turbulent heat flux forcing (Figure 4b). Very similar results are found using turbulent flux estimates from individual observational data sets (Figure S7).

On interannual timescales, North Atlantic variability is therefore also driven by mechanisms that exhibit pronounced spatial heterogeneity. Heating of the subtropical NE Atlantic typical of North Atlantic variability's growth phase is driven primarily by surface turbulent heat flux. Heating of the midlatitude NE Atlantic is driven primarily by oceanic processes—specifically advection. We find very little role for anomalous cloud radiative flux for North Atlantic variability, unlike for North Pacific variability. This might reflect the more limited coverage of stratocumulus clouds in the NE Atlantic relative to the NE Pacific. Moreover, these results provide observational evidence in support of recent cloud-locking experiments that show a weak impact of cloud radiative feedbacks on SST variance in the subtropical NE Atlantic relative to that in the subtropical NE Pacific (Middlemas et al., 2019).

The large-scale spatial patterns of the relative contributions of different heat fluxes to the local heat content tendency associated with the growth phase of North Atlantic variability are consistent with these results (Figure S8). But the patterns also show that the impacts of individual processes on upper ocean heating can locally deviate from their contributions on a large scale. Notably, the contribution of F'_{cloud} to anomalous heating of the mixed layer approaches isolated values of up to ~45% near 320°E and 12°N and that of F'_{ocean} approaches ~100% along the coasts of Africa and the Iberian Peninsula. The latter result suggests that upwelling is crucial for inducing coastal SST anomalies associated with North Atlantic variability.

5. Discussion and Conclusions

Our observational results demonstrate that the interannual SST anomaly pattern characteristic of North Pacific variability is produced by a mix of atmospheric, oceanic, and coupled processes with a high degree of spatial heterogeneity. SST anomalies associated with the warm phase of North Pacific variability are amplified during periods when the Aleutian Low is strengthened. In the midlatitude North Pacific, strengthened westerlies during the warm phase of North Pacific variability increase Ekman-driven equatorward cold advection and, to a lesser extent, ocean-to-atmosphere turbulent heat flux, cooling the ocean. In the subtropical NE Pacific, weakened trade winds associated with a stronger Aleutian Low reduce the ocean-to-atmosphere turbulent heat flux and vertical mixing at the base of the mixed layer, warming the ocean. In this region, a reduction in the cooling cloud radiative effect also occurs, warming the ocean by an amount comparable to that due to anomalous turbulent flux or vertical mixing. Around half of this reduction is inferred to be a result of a cloud radiative feedback. Cloud radiative flux anomalies hence provide a major source of interannual SST variability in this region, consistent with previous modeling studies (Bellomo et al., 2014; Burgman et al., 2017; Middlemas et al., 2019) and the observational findings of Myers, Mechoso, Cesana, et al. (2018) on mechanisms for the 2014–2015 marine heatwave off Baja California.

In contrast, we find that the impact of cloud radiative flux anomalies on the large-scale pattern of interannual SST anomalies characteristic of North Atlantic variability is very small relative to other processes. In particular, SST anomalies associated with the warm phase of North Atlantic variability are amplified during periods of anomalous cyclonic circulation over the North Atlantic. In this configuration, weakened background winds in the subtropical NE Atlantic and midlatitude NE Atlantic decrease the ocean-to-atmosphere turbulent heat flux, warming the ocean. Weaker westerlies in the midlatitude NE Atlantic also reduce Ekman-driven equatorward cold advection, warming the ocean by an amount even larger than that due to anomalous turbulent flux. The dominance of turbulent and oceanic fluxes in our observational analysis does not preclude the importance of cloud radiative anomalies for North Atlantic SST variations in particular seasons or on decadal timescales, as previous studies have found (Bellomo et al., 2016; Myers, Mechoso, & DeFlorio, 2018; Yuan et al., 2016; Yuan et al., 2018). But it does suggest that the leading pattern of interannual SST variability in the North Atlantic is almost entirely modulated by other processes.

Acknowledgments
This work was performed under the auspices of the U.S. Department of Energy (DOE) by Lawrence Livermore National Laboratory under Contract DE-AC52-07NA27344. T. A. M. was supported in part by LLNL Institutional Postdoctoral Program and by NOAA's Climate Program Office, Climate Variability and Predictability Program Award NA14OAR4310278 at UCLA. Data used in the study are available for download online (https://www.esrl.noaa.gov/psd/data/gridded/ [NOAA OI SST and GODAS], http://research.jisao.washington.edu/pdo/PDO.latest.txt [PDO index], https://ceres.larc.nasa.gov/ [CERES-EBAF], http://oaflux.whoi.edu [OAFlux], http://apps.ecmwf.int/datasets/ [ERA-I], https://rda.ucar.edu/ [CFSR], and https://disc.gsfc.nasa.gov/ [MERRA-2]). The authors wish to thank two anonymous reviewers for their efforts in helpfully commenting on the paper.

References

Battisti, D. S., Bhatt, U. S., & Alexander, M. A. (1995). A modeling study of the interannual variability in the wintertime North Atlantic Ocean. *Journal of Climate*, *8*(12), 3067–3083.

Behringer, D. W. (2007). The Global Ocean Data Assimilation System (GODAS) at NCEP, paper 3.3 presented at 11th Symp. on Integrated Observing and Assimilation Systems for Atmosphere, Oceans, and Land Surface, Am. Meteorol. Soc., San Antonio, Tex., Preprints. Retrieved from http://ams.confex.com/ams/87ANNUAL/techprogram/paper_119541.htm

Behringer, D. W., & Xue, Y. (2004). Evaluation of the Global Ocean Data Assimilation System at NCEP: The Pacific Ocean, paper 2.3 presented at Eighth Symp. on Integrated Observing and Assimilation Systems for Atmosphere, Oceans, and Land Surface, Am. Meteorol. Soc., Seattle, Wash., Preprints. Retrieved from http://ams.confex.com/ams/84Annual/techprogram/paper_70720.htm

Bellomo, K., Clement, A., Mauritsen, T., Rädel, G., & Stevens, B. (2014). Simulating the role of subtropical stratocumulus clouds in driving Pacific climate variability. *Journal of Climate*, *27*(13), 5119–5131. https://doi.org/10.1175/JCLI-D-13-00548.1

Bellomo, K., Clement, A. C., Murphy, L. N., Polvani, L., & Cane, M. A. (2016). New observational evidence for a positive cloud feedback that amplifies the Atlantic Multidecadal Oscillation. *Geophysical Research Letters*, *43*, 9852–9859. https://doi.org/10.1002/2016GL069961

Bosilovich, M. G., Mocko, D., Roads, J. O., & Ruane, A. (2009). A multimodel analysis for the Coordinated Enhanced Observing Period (CEOP). *Journal of Hydrometeorology*, *10*(4), 912–934.

Bretherton, C. S., Blossey, P. N., & Jones, C. R. (2013). Mechanisms of marine low cloud sensitivity to idealized climate perturbations: A single-LES exploration extending the CGILS cases. *Journal of Advances in Modeling Earth Systems*, *5*(2), 316–337. https://doi.org/10.1002/jame.20019

Brown, P. T., Lozier, M. S., Zhang, R., & Li, W. (2016). The necessity of cloud feedback for a basin-scale Atlantic Multidecadal Oscillation. *Geophysical Research Letters*, *43*, 3955–3963. https://doi.org/10.1002/2016GL068303

Burgman, R. J., Clement, A. C., Mitas, C. M., Chen, J., & Esslinger, K. (2008). Evidence for atmospheric variability over the Pacific on decadal timescales. *Geophysical Research Letters*, *35*(1).

Burgman, R. J., Kirtman, B. P., Clement, A. C., & Vazquez, H. (2017). Model evidence for low-level cloud feedback driving persistent changes in atmospheric circulation and regional hydroclimate. *Geophysical Research Letters*, *44*, 428–437. https://doi.org/10.1002/2016GL071978

Cayan, D. R. (1992). Latent and sensible heat flux anomalies over the northern oceans: Driving the sea surface temperature. *Journal of Physical Oceanography*, *22*(8), 859–881.

Clement, A., Bellomo, K., Murphy, L. N., Cane, M. A., Mauritsen, T., Rädel, G., & Stevens, B. (2015). The Atlantic Multidecadal Oscillation without a role for ocean circulation. *Science*, *350*(6258), 320–324. https://doi.org/10.1126/science.aab3980

Clement, A. C., Burgman, R., & Norris, J. R. (2009). Observational and model evidence for positive low-level cloud feedback. *Science*, *325*(5939), 460–464. https://doi.org/10.1126/science.1171255

Dee, D. P., Uppala, S. M., Simmons, A. J., Berrisford, P., Poli, P., Kobayashi, S., et al. (2011). The ERA-Interim reanalysis: Configuration and performance of the data assimilation system. *Q. J. R. Meteorol. Soc.*, *137*(656), 553–597.

Deser, C., Alexander, M. A., Xie, S. P., & Phillips, A. S. (2010). Sea surface temperature variability: Patterns and mechanisms. *Annual review of marine science*, *2*, 115–143. https://doi.org/10.1146/annurev-marine-120408-151453

Deser, C., Phillips, A. S., & Hurrell, J. W. (2004). Pacific interdecadal climate variability: Linkages between the tropics and the North Pacific during boreal winter since 1900. *Journal of Climate*, *17*(16), 3109–3124.

Frankignoul, C., & Hasselmann, K. (1977). Stochastic climate models, Part II Application to sea-surface temperature anomalies and thermocline variability. *Tellus*, *29*(4), 289–305.

Frankignoul, C., & Kestenare, E. (2002). The surface heat flux feedback. Part I: Estimates from observations in the Atlantic and the North Pacific. *Climate dynamics*, *19*(8), 633–647.

Gelaro, R., McCarty, W., Suárez, M. J., Todling, R., Molod, A., Takacs, L., et al. (2017). The modern-era retrospective analysis for research and applications, version 2 (MERRA-2). *Journal of Climate*, *30*(14), 5419–5454.

Gleckler, P. J., Taylor, K. E., & Doutriaux, C. (2008). Performance metrics for climate models. *Journal of Geophysical Research: Atmospheres*, *113*(D6).

Hausmann, U., Czaja, A., & Marshall, J. (2016). Estimates of air–sea feedbacks on sea surface temperature anomalies in the Southern Ocean. *Journal of Climate*, *29*(2), 439–454.

Kato, S., Rose, F. G., Rutan, D. A., Thorsen, T. J., Loeb, N. G., Doelling, D. R., et al. (2018). Surface irradiances of edition 4.0 clouds and the Earth's Radiant Energy System (CERES) Energy Balanced and Filled (EBAF) data product. *Journal of Climate*, *31*, 4501–4527.

Klein, S. A., Hall, A., Norris, J. R., & Pincus, R. (2017). Low-cloud feedbacks from cloud-controlling factors: A review. *Surveys in Geophysics*, 1–23.

Klein, S. A., & Hartmann, D. L. (1993). The seasonal cycle of low stratiform clouds. *Journal of Climate, 6*(8), 1587–1606. https://doi.org/10.1175/1520-0442(1993)006<1587:TSCOLS>2.0.CO;2

Middlemas, E., Clement, A., & Medeiros, B. (2019). Contributions of atmospheric and oceanic feedbacks to subtropical northeastern sea surface temperature variability. *Climate Dynamics.*, *53*(11), 6877–6890. https://doi.org/10.1007/s00382-019-04964-1

Myers, T. A., Mechoso, C. R., Cesana, G. V., DeFlorio, M. J., & Waliser, D. E. (2018). Cloud feedback key to marine heatwave off Baja California. *Geophysical Research Letters*, *45*(9), 4345–4352.

Myers, T. A., Mechoso, C. R., & DeFlorio, M. J. (2018). Coupling between marine boundary layer clouds and summer-to-summer sea surface temperature variability over the North Atlantic and Pacific. *Climate Dynamics*, *50*(3-4), 955–969. https://doi.org/10.1007/s00382-017-3651-8

Newman, M., Alexander, M. A., Ault, T. R., Cobb, K. M., Deser, C., Di Lorenzo, E., et al. (2016). The Pacific Decadal Oscillation, revisited. *Journal of Climate*, *29*(12), 4399–4427.

Norris, J. R., Zhang, Y., & Wallace, J. M. (1998). Role of low clouds in summertime atmosphere–ocean interactions over the North Pacific. *Journal of Climate*, *11*(10), 2482–2490.

Park, S., Deser, C., & Alexander, M. A. (2005). Estimation of the surface heat flux response to sea surface temperature anomalies over the global oceans. *Journal of climate*, *18*(21), 4582–4599.

Reynolds, R. W., Rayner, N. A., Smith, T. M., Stokes, D. C., & Wang, W. (2002). An improved in situ and satellite SST analysis for climate. *Journal of Climate*, *15*(13), 1609–1625. https://doi.org/10.1175/1520-0442(2002)015<1609:AIISAS>2.0.CO;2

Rieck, M., Nuijens, L., & Stevens, B. (2012). Marine boundary layer cloud feedbacks in a constant relative humidity atmosphere. *Journal of the Atmospheric Sciences*, *69*(8), 2538–2550. https://doi.org/10.1175/JAS-D-11-0203.1

Saha, S., Moorthi, S., Pan, H. L., Wu, X., Wang, J., Nadiga, S., et al. (2010). The NCEP climate forecast system reanalysis. *Bull. Am. Meteorol. Soc.*, *91*, 1015–1057.

van der Dussen, J. J., de Roode, S. R., Gesso, S. D., & Siebesma, A. P. (2015). An LES model study of the influence of the free troposphere on the stratocumulus response to a climate perturbation. *Journal of Advances in Modeling Earth Systems*, *7*(2), 670–691. https://doi.org/10.1002/

Yu, L., Jin, X., & Weller, R. A. (2008). Multidecade global flux datasets from the objectively analyzed air-sea fluxes (OAFlux) project: Latent and sensible heat fluxes, ocean evaporation, and related surface meteorological variables, Tech. Rep. OA-2008-01, Woods Hole Oceanogr. Inst., Woods Hole, Mass.

Yuan, T., Oreopoulos, L., Platnick, S. E., & Meyer, K. (2018). Observations of local positive low cloud feedback patterns and their role in internal variability and climate sensitivity. *Geophysical Research Letters*, *45*(9), 4438–4445. https://doi.org/10.1029/2018GL077904

Yuan, T., Oreopoulos, L., Zelinka, M., Yu, H., Norris, J. R., Chin, M., et al. (2016). Positive low cloud and dust feedbacks amplify tropical North Atlantic Multidecadal Oscillation. *Geophysical Research Letters*, *43*(3), 1349–1356.

Zhang, Y. C., Rossow, W. B., & Lacis, A. A. (1995). Calculation of surface and top of atmosphere radiative fluxes from physical quantities based on ISCCP data sets: 1. Method and sensitivity to input data uncertainties. *Journal of Geophysical Research: Atmospheres*, *100*(D1), 1149–1165.